Limnol. Oceanogr., 48(3), 2003, 1277–1288

Cryptic coloration and mirrored sides as camouflage strategies in near-surface pelagic habitats: Implications for foraging and predator avoidance

Sönke Johnsen[1]
Biology Department, P.O. Box 90338, Duke University, Durham, North Carolina, 27708

Heidi M. Sosik
Biology Department, Woods Hole Oceanographic Institution, Woods Hole, Massachusetts, 02543

Abstract

Mirrored and colored surfaces are common adaptations for crypsis in pelagic habitats. Although highly successful when optimized for a particular situation, either may become less successful if it is then viewed in a different situation. In this study we examine the relative robustness of these two strategies by determining how visible an organism becomes when viewed under optical conditions different from those under which the camouflage is optimal. Underwater radiance distributions were calculated using inherent optical properties measured in coastal waters 80 km off the coast of New Hampshire. These radiance distributions were then used to calculate optimally cryptic diffuse and specular reflectance spectra as a function of depth, solar elevation, viewing angle, and azimuth. Then the visibilities of organisms cryptic in one situation viewed in a different situation were calculated, using the Atlantic Cod, *Gadus morhua,* as the viewer. In contrast to benthic organisms, pelagic organisms cryptic under one set of optical conditions were quite visible under a different set, particularly when viewed from a different azimuth. The crypsis afforded by mirrored surfaces was generally more robust than that resulting from colored surfaces. However, because mirrored surfaces could never be perfectly cryptic when viewed in the azimuth of the sun, neither strategy clearly outperformed the other. In general, crypsis by colored or mirrored surfaces was not robust in near-surface water, which may help explain both the predominance of transparent species in near-surface pelagic habitats and the vertical migration of many colored and mirrored species. The results also show that three common foraging strategies—circling, crepuscular activity, and driving prey toward the surface—all increase the visibility of cryptically colored or mirrored prey.

Although establishing an evolutionary link between a trait and its adaptive function is notoriously difficult, it is generally accepted that tissue transparency, counterillumination, mirrored sides, and countershading are all major adaptations for crypsis in the pelagic environment (Denton et al. 1972; Herring and Roe 1988; Johnsen 2001). All are highly successful when the organism is viewed under the conditions for which the strategy is optimized. However, the different strategies may vary in their ability to accommodate to a different set of optical conditions. Though not well studied, the importance of changing optical conditions on aquatic crypsis has been previously noted (e.g., Barry and Hawryshyn 1999; Marshall 2000).

A transparent organism accommodates trivially to changing conditions by simply transmitting the background light (Johnsen 2001). Many counterilluminating organisms are known to alter the intensity, angular distribution, and spectrum of their emitted light to remain cryptic over a wide range of optical environments (Denton et al. 1972). Certain colored and mirrored pelagic organisms are known to change color in an apparent cryptic response to changing optical conditions (e.g., Denton 1970; Herring and Roe 1988; Endler 1991), but cryptic color changes and the potential need for them remain poorly understood for pelagic species.

The current study examines how robust cryptic coloration and mirroring are under varying optical and viewing conditions. First, the ideally cryptic reflectances for organisms in coastal water are calculated for a variety of optical conditions. Then, using the Atlantic Cod *Gadus morhua* as the viewer, the sighting distances of organisms optimally cryptic in one condition, but viewed in another, are determined. The overall goal is to determine the relative success of the two cryptic strategies when faced with a varying optical environment and to determine the potential importance of the ability to change color.

Materials and methods

Modeling underwater visibility—According to Johnsen (2002), the maximum distance at which a large organism can be detected (referred to hereafter as the sighting distance) is

$$d(\lambda) = \frac{\ln\left[\frac{|C_o(\lambda)|}{C_{\min}(\lambda)}\right]}{c(\lambda) - K_L(\lambda)} \quad (1)$$

where $C_o(\lambda)$ is the contrast of the organism when viewed from a short distance (referred to hereafter as the inherent

[1] Corresponding author.

Acknowledgments

The authors thank Thomas Cronin, Tamara Frank, Dina Leech, and Edith Widder for comments on the manuscript. This work was funded in part by a grant from the National Science Foundation (OCE-011844) to Laurence P. Madin and S.J. and by NASA grant NAG5-8868 and ONR grant N00014-01-10256 to H.M.S. This is Contribution No. 10670 of the Woods Hole Oceanographic Institution.

contrast), $C_{\min}(\lambda)$ is the minimum contrast for large object detection for a given visual system, $c(\lambda)$ is the beam attenuation coefficient of the water, and $K_L(\lambda)$ is the attenuation coefficient of the background radiance. Note that $K_L(\lambda)$ depends strongly on viewing angle, being greatest for downward viewing and zero for horizontal viewing (Johnsen 2002). However, when an organism subtends an angle less than a certain critical angle on the viewer's visual field, its visibility also depends on its apparent area A, which is inversely proportional to the square of distance (Anthony 1981; Aksnes and Utne 1997). This factor can be included in the standard contrast attenuation equations by making the minimum contrast threshold a function of distance:

$$C_{\min}(\lambda, d) = \begin{cases} C_{\min}(\lambda) & \text{if } d \le d_c \quad \text{and} \\ C_{\min}(\lambda)\dfrac{d^2}{d_c^2} & \text{if } d > d_c \end{cases} \tag{2}$$

where d_c is the distance at which the organism subtends the critical angle on the viewer's visual field (i.e., the distance at which it becomes ''small'') and $C_{\min}(\lambda)$ is the minimum contrast threshold for objects closer than d_c. Therefore, for ''small'' organisms:

$$d(\lambda) = \frac{\ln\left[\dfrac{|C_o(\lambda)|}{C_{\min}(\lambda)} \cdot \dfrac{d_c^2}{d^2(\lambda)}\right]}{c(\lambda) - K_L(\lambda)} \tag{3}$$

which cannot be solved analytically, but which is easily solved by iteration. Note that Eq. 3 is only valid when $d > d_c$. When $d \le d_c$, Eq. 1 must be used.

Although the background radiance is relatively easy to model or measure, the radiance of an arbitrary object is a complex function of the light field incident on it and its reflectance properties. The reflectance of light from objects ranges from being completely diffuse (lambertian) to highly ordered (specular or mirrorlike). In this study, we examine these two extremes. Although no biological surface is perfectly lambertian or specular, they can be considered as opposing strategies toward which organismal reflectances can evolve. For clarity, lambertian reflection will be referred to hereafter as diffuse reflection for the remainder of this article.

The radiance of an organism that reflects light diffusely is equal to $[R(\lambda)E(\lambda)]/\pi$, where $R(\lambda)$ is reflectance and $E(\lambda)$ is the irradiance at the surface of the organism (Johnsen 2002). This radiance matches the background radiance $L_b(\lambda)$ when

$$R(\lambda) = \frac{\pi L_b(\lambda)}{E(\lambda)} \quad \text{(Fig. 1a)} \tag{4}$$

Non-lambertian diffuse reflectors generally reflect less light over large angles than true lambertian reflectors (Palmer 1995). Therefore, the non-lambertian nature of actual organisms will mostly influence the predictions for lateral surface crypsis at high solar elevations, because less light from the overhead sun will reflect to the viewer than predicted. In this case, the predicted cryptic reflectance will likely underestimate the correct value. For organisms that reflect light specularly and are viewed horizontally, their radiance matches the background when the specular reflectance equals

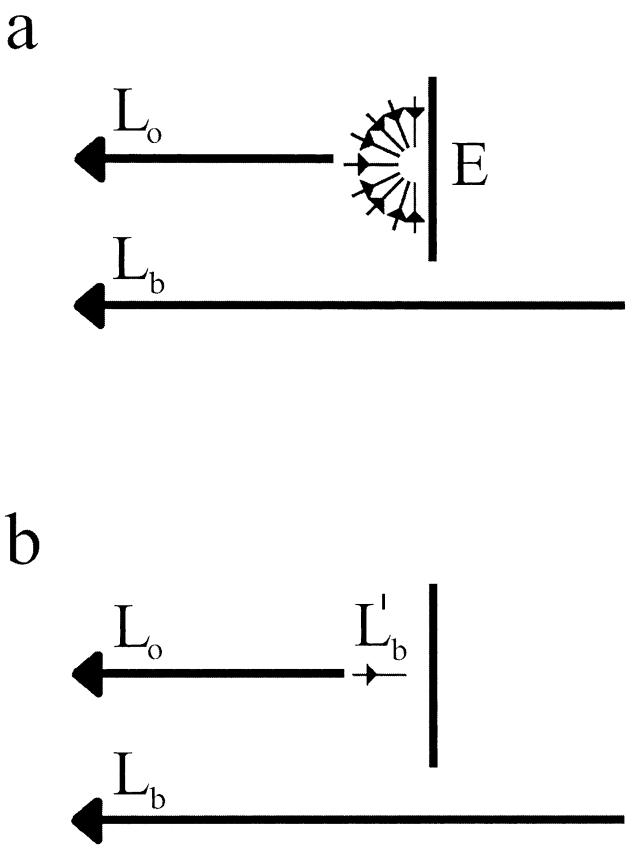

Fig. 1. Two surfaces viewed horizontally. a) A diffusely reflective (colored) surface. The radiance of the surface, L_0, is equal to RE/π, where R is the diffuse reflectance and E is the irradiance at the surface (depicted by the cluster of inward pointing arrows). b) a specularly reflective (mirrored) surface. The radiance of the surface is equal to RL'_b, where L'_b is the radiance in the opposite azimuth from the line of sight (depicted by the small arrow).

$$R_{\text{specular}}(\lambda) = \frac{L_b(\lambda)}{L'_b(\lambda)} \tag{5}$$

where $L'_b(\lambda)$ is the background radiance in the opposite azimuth of $L_b(\lambda)$ (Fig. 1b).

In the current study, three different viewing angles were examined: (1) viewing from directly above, (2) viewing horizontally in the solar azimuth, and (3) viewing horizontally opposite the solar azimuth. Because the dorsal surfaces of aquatic organisms are rarely mirrored, the first viewing angle was only examined for diffusely reflecting surfaces. In addition, viewing from below was not studied because preliminary results showed that the downwelling light was far too bright for any coloring or mirroring of the ventral surface to have any significant cryptic benefit (as was also found in Johnsen [2002]).

For each viewing angle, the viewed surface was assumed to be perpendicular to the viewing angle. Obviously, no organism is shaped like a cube. However, pelagic nekton, with the exception of top predators such as sharks, large scombrids, and cetaceans, are generally compressed, with flat lat-

eral surfaces and limited regions of curvature (Denton 1970). Nevertheless, curvature can play an important role, particularly in mirrored organisms near the surface (see Discussion).

Calculation of underwater radiances and irradiances—The underwater light field was modeled using measured inherent optical properties of the water (IOPs) and radiative transfer software (Hydrolight 4.1, Sequoia Scientific) (see Mobley et al. [1993] and Johnsen [2002] for further details and justification). Depth profiles of inherent optical properties were measured using a dual path, multiband absorption/attenuation meter (ac-9, WETLabs) and backscattering meters (a-βeta and HydroScat-2, HOBILabs) at a site 80 km from the coast of Portsmouth, New Hampshire (42°47′N 70°05′W, 1106 h local time, 30 June 2000). Measurements were corrected for temperature and salinity, and absorption measurements were corrected for scattering errors (Zaneveld et al. 1994; Pegau et al. 1997). The backscattering meters were calibrated by the manufacturer, and the ac-9 was calibrated on its deployment frame using water generated with a Milli-Q purification system (Millipore Corp.). Absorption and beam attenuation coefficients (at 440, 488, 510, 532, 555, and 650 nm) and backscattering coefficients (at 442, 470, 488, and 676 nm) were averaged over 1-m intervals to a depth of 92 m. All data were collected on upcasts to limit artifacts due to bubbles, etc. In addition, discrete samples were collected from three depths (1, 20, and 40 m), filtered onto Whatman GF/F filters, and extracted overnight in cold 90% acetone for standard fluorometric determination of chlorophyll concentration.

Underwater radiance distributions were calculated from 0- to 50-m depth at 5-m intervals for two solar elevations, 10° and 80°, chosen to approximate two extremes of skylight radiance distribution. For each distribution, the sky and sea were considered to be cloudless and calm, respectively. The sky irradiance was calculated using the Radtran model (Gregg and Carder 1990), and the sky radiance distribution was calculated using the model given in Harrison and Coombes (1988). Pure water absorption was taken from Pope and Fry (1997). The scattering phase function was a Fournier–Forand function chosen to fit the measured backscatter ratio (Mobley et al. 2002). Chlorophyll fluorescence was calculated from chlorophyll absorption estimated according to Prieur and Sathyendranath (1981) and a fluorescence efficiency of 0.02.

At each depth, radiance was calculated from 400 to 620 nm at 15-nm intervals with an angular resolution of 15° (azimuth) by 10° (elevation). *G. Morhua* has no significant visual sensitivity above 620 nm (Anthony and Hawkins 1983). From the radiance distributions, irradiances were calculated for the following vectors: downward, horizontal in the solar azimuth, and horizontal opposite the solar azimuth. The irradiances and radiances appropriate for the three viewing angles were inserted in to Eqs. 4 and 5 to determine the optimally cryptic diffuse and specular reflectances.

Measurements of direct upward radiance and downwelling irradiance—Downwelling irradiance and upward radiance data were taken concurrently with the IOP profiles described above. Three profiles were obtained using a multispectral radiometer (SPMR, Satlantic) that simultaneously measured downwelling irradiance and upward radiance (at 412, 443, 490, 510, and 554 nm). The bandwidth of the filters was 10 nm (full width, half maximum). The measurements that were above the noise level of the instrument were inserted into Eq. 4 to compare with the modeled prediction for cryptic diffuse reflectance when viewed from above.

Prediction of sighting distances of organisms cryptic in one situation viewed in a different situation—Four mismatch conditions were examined: (1) an organism cryptic in oceanic water that is viewed in coastal water, (2) an organism cryptic near noon (solar elevation 80°) that is viewed near sunset (solar elevation 10°), (3) an organism cryptic in one azimuth that is viewed horizontally in the opposite azimuth, and (4) an organism cryptic at 50 m depth that is viewed at shallower depths. The viewer was chosen to be the Atlantic Cod, *G. morhua*, because it is found at the studied depths in New England coastal waters and because its spectral sensitivity and contrast thresholds at the given range of light intensities are known (Anthony 1981; Anthony and Hawkins 1983). Although adult cod are generally associated with the sea floor, larval and juvenile cod are pelagic, with a primarily pelagic diet (Link and Garrison 2002).

The inherent contrast of a diffusely reflecting surface at a wavelength λ is

$$C_o(\lambda) = \frac{L_o}{L_b} - 1 \cong \frac{R(\lambda)E(\lambda)}{\pi L_b(\lambda)} - 1 \tag{6}$$

where $R(\lambda)$ is the diffuse reflectance of the surface and $E(\lambda)$ and $L_b(\lambda)$ are again the irradiance and background radiance, respectively (Johnsen 2002). Visual systems perceive two forms of contrast; chromatic contrast (e.g., red on green) and brightness contrast (e.g., red on dark red). This study limits itself to brightness contrast because although color vision is known in many aquatic species, chromatic contrast is well understood in only a few model systems, none of which are pelagic. This limitation implies that the predicted sighting distances may underestimate the true values, because hue discrimination is not considered. However, hue discrimination becomes increasingly less useful with increasing depth, even in clear water (Chiao et al. 2000). Also, note that a color mismatch can result in brightness contrast, as can readily be seen in black and white images. The perceived brightness contrast for *G. morhua* is equal to Eq. 7 integrated over and weighted by its photopic spectral sensitivity:

$$C_o = \frac{\int R(\lambda)E(\lambda)V(\lambda)\,d\lambda}{\pi \int L_b(\lambda)V(\lambda)\,d\lambda} - 1 \tag{7}$$

where $V(\lambda)$ is the photopic spectral response curve of cod taken from Anthony and Hawkins (1983) (the study depths are all within the photopic region of the cod visual system). The minimum contrast threshold of cod has been measured

as a function of the background illumination (Anthony 1981) and at photopic intensities was closely approximated by:

$$C_{\min} = 0.0129 \cdot L_b^{-0.111} \quad (8)$$

where L_b is the background radiance integrated over the photopic sensitivity of the cod ($R^2 > 0.995$ for regression). Therefore, the minimum contrast threshold rises with increasing depth.

To determine the sighting distance d exactly, one must also include the spectral dependence of the beam and diffuse attenuation coefficients of the water, which involves solving

$$C_{\min} = \frac{\int e^{-c(\lambda)d}\left[\frac{R(\lambda)E(\lambda)}{\pi} - L_b^0(\lambda)\right]V(\lambda)\,d\lambda}{\int L_b^d(\lambda)V(\lambda)\,d\lambda} \quad (9)$$

for d, where $L_b^0(\lambda)$ and $L_b^d(\lambda)$ are the background radiances at distances zero and d from the organism (adapted from Mertens 1970). This equation is generally not analytically solvable and is certainly not easy to interpret. However, preliminary results showed that the sighting distance for large organisms was closely approximated by substituting Eqs. 7 and 8 into Eq. 1 and using the beam and radiance attenuation coefficients at 440 nm, the wavelength of peak visual sensitivity (Anthony and Hawkins 1983) (see Results). The sighting distance for small organisms was calculated by substituting Eqs. 7 and 8 into Eq. 3 and solving for sighting distance by iteration. The critical angle for cod is unknown, so, following arguments from Anthony (1981), it was set at 200 min of an arc (approximately 3°). The ''large'' organism was chosen to be 1 m long, so its apparent size was above the critical angle at viewing distances as long as 17 m. The ''small'' organism was chosen to be 6 mm long; thus, its apparent size fell below the critical angle at a viewing distance of 10 cm. The two size classes can be thought of as predators and prey of pelagic cod, respectively.

All the previous calculations were performed for specularly reflective surfaces by substituting $L_b'(\lambda)$ for $E(\lambda)/\pi$ in Eqs. 6 through 9. The reflectances of organisms that are cryptic in oceanic water (condition 1) were taken from Johnsen (2002). All other reflectances were taken from the current study. The beam attenuation coefficients, $c(\lambda)$, were obtained from the measured attenuation profiles. The coefficients of background radiance attenuation, $K_L(\lambda)$, were determined from the calculated radiance distributions.

Sighting distances were calculated at 0-, 5-, 10-, 20-, 30-, and 50-m depths, except for condition 1, where the 5-m depth was excluded because of a lack of oceanic data at this depth. The downward and the two horizontal viewing angles were examined in conditions 1 and 2 and 4, respectively. Only the horizontal viewing angles were examined for specularly reflective surfaces.

Results

Modeled downwelling and upwelling irradiance—The calculated irradiances and radiances in all four viewing angles displayed a peak at approximately 570 nm, with significantly higher attenuation at both longer and shorter wavelengths as a result of phytoplankton absorption (Fig. 2). The modeled spectra near sunset (solar elevation of 10°) had values approximately 1/10 of those near noon (solar elevation of 80°). In addition, the light field was more asymmetrical near the surface, with higher radiance in the solar azimuth. The measured upward radiance and downwelling irradiance approximated the modeled radiance and irradiance (Fig. 2), although with a peak at a shorter wavelength. At all wavelengths, the measured radiance and irradiance data displayed the same pattern of discrepancies relative to the modeled data (e.g., modeled radiance and irradiance at 555 nm are both higher than what is measured). Therefore, the modeled ratios of radiance to irradiance (which determine the predicted reflectances) matched the measured ratios quite closely.

The radiances weighted by the visual response curve of *G. morhua* show that, near the surface, wavelengths near the animal's visual response peak contributed the most to brightness perception (Fig. 2c,d). At greater depths, the wavelengths neighboring the 570-nm illumination peak dominated the brightness perception.

Predicted reflectance for maximal crypsis—For an organism viewed from above near noon, the predicted diffuse reflectance spectra from 400 to 575 nm increased slightly with depth and had a broad double peak centered at 525 nm (Fig. 3a). For wavelengths greater than 575 nm, the predicted reflectance increased from a relatively low value at the surface to approximately 0.27 at a depth of 50 m. The reflectance spectra predicted from the profiles of downwelling irradiance and upward radiance closely approximated those from the modeled light field (Fig. 3b). The predicted reflectances near sunset were similar to those predicted near noon (not shown).

For organisms viewed horizontally near noon in the solar azimuth, the predicted diffuse reflectances were relatively high, with a broad peak centered at 575 nm (Fig. 3c). With increasing depth, long wavelength reflectance increased to a maximum of approximately 0.8. For organisms viewed opposite the solar azimuth (i.e., with the sun behind the viewer), the pattern was similar to that noted for organisms viewed from above, with the lowest predicted reflectance measuring approximately 10-fold greater (Fig. 3d). Near sunset, the predicted near-surface reflectances were higher in the solar azimuth and lower opposite the solar azimuth because of the asymmetrical light field (not shown). At depth, the differences were less pronounced.

For specularly reflective organisms viewed horizontally near noon, the predicted reflectance was slightly greater than one when viewed in the solar azimuth and slightly less than one when viewed opposite the solar azimuth (Fig. 4a,b). The reflectance was relatively independent of depth. Near sunset, the predicted reflectances ranged from ¼ to 4, depending on depth and azimuth, with the greatest departures from 100% reflectance seen at shallow depths (Fig. 4c,d).

Sighting distances of large organisms cryptic in one situation viewed in a different situation—The sighting distance of a diffusely reflective, cryptic, oceanic organism viewed in coastal water was relatively independent of depth and

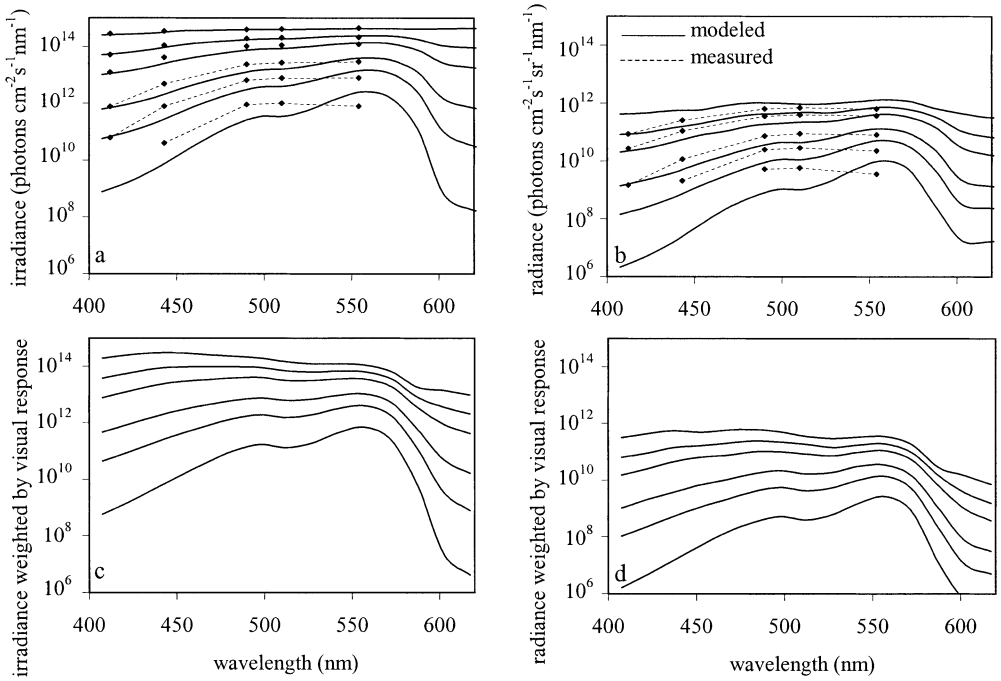

Fig. 2. a) Modeled and measured downwelling irradiance. b) Modeled and measured direct upward radiance. c) Modeled downwelling irradiance weighted by the visual response curve of *G. morhua.* d) Modeled direct upward radiance weighted by the visual response curve of *G. morhua.* Depths are 0, 5, 10, 20, 30, and 50 m, and solar elevation equals 80°. Measurements were taken at 1106 h local time and adjusted so that surface irradiance matched the modeled surface irradiance. Radiance and irradiance values below the noise level of the radiometer are not shown. There is no measurement for direct upward radiance at 0 m. Due to the weighting factor, the y-axis in c and d has arbitrary units.

viewing angle, with an average value of approximately 10 m (Fig. 5a). The sighting distance of an organism cryptic at noon viewed at sunset depended strongly on viewing angle (Fig. 5b). When viewed from above, the sighting distance was generally negligible. When viewed horizontally in the solar azimuth, the sighting distance ranged from 0 to 5 m, depending on depth. When viewed horizontally opposite the solar azimuth, the sighting distance decreased from 8 m at the surface to a negligible value at a depth of 50 m. Diffusely reflective organisms cryptic in one azimuth viewed in the opposite azimuth at the same time of day had the longest sighting distances of any mismatch condition (Fig. 5c,d). The sighting distances at noon ranged from 8 to 20 m depending on depth and viewing azimuth. The sighting distances near sunset were somewhat shorter but followed the same general depth profile. At both times of day, organisms cryptic opposite the solar azimuth viewed in the solar azimuth had somewhat shorter sighting distances overall, compared to organisms cryptic in the solar azimuth viewed opposite the solar azimuth. Diffusely reflective organisms cryptic at 50-m depth had sighting distances ranging from 0 to 12 m at shallower depths (Fig. 5e,f). The sighting distances were generally longer at shallower depths, though the pattern for organisms viewed in the solar azimuth was complex. The sighting distances at the two solar elevations were generally comparable, with horizontal sighting distances being larger than downward viewing distances.

For specularly reflective organisms, the patterns were quite similar to those determined for diffusely reflective organisms, but the magnitudes of the sighting distances differed (Fig. 6). The sighting distances for oceanic organisms viewed in coastal water were significantly lower (Fig. 6a), as were the sighting distances for organisms cryptic in one azimuth viewed in the opposite azimuth (Fig. 6c,d). The sighting distances for organisms cryptic near noon viewed at sunset were higher, however (Fig. 6b). For organisms cryptic at 50-m depth viewed at shallower depths, specularly reflective organisms had lower sighting distances near noon and higher sighting distances near sunset (Fig. 6e,f).

Sighting distances of small organisms cryptic in one situation viewed in a different situation—The sighting distances of both diffusely and specularly reflective small organisms were inversely proportional to depth, generally with a linear relationship. Cryptic oceanic organisms viewed in coastal water had relatively high sighting distances that were significantly higher for diffusely reflective organisms than for specularly reflective organisms (Table 1). Organisms cryptic at noon viewed at sunset had relatively low sighting distances that depended strongly on viewing angle but were relatively independent of the form of the reflectance. Organisms cryptic in one azimuth viewed in the opposite azimuth at the same time of day had the longest sighting distances of any of the conditions, particularly in the diffusely reflec-

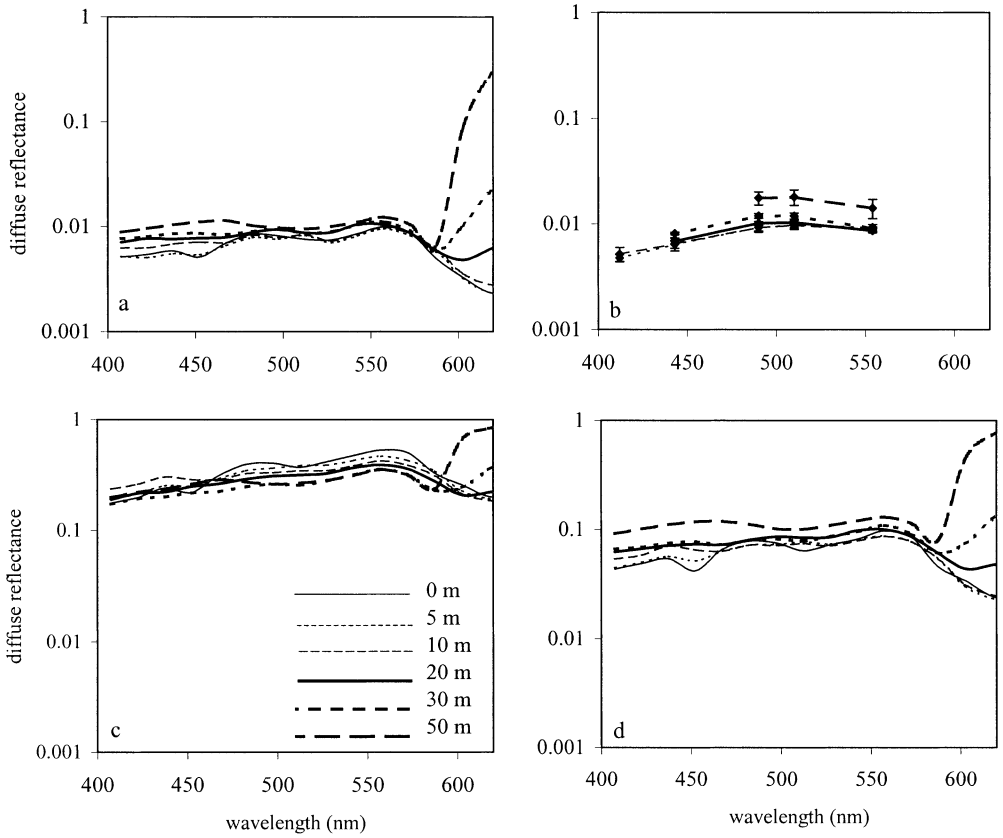

Fig. 3. Predicted diffuse reflectance spectra of a maximally cryptic organism. a) Predicted reflectance of the dorsal surface of an organism viewed from above using modeled light field. b) Predicted reflectance of the dorsal surface of an organism viewed from above using three vertical profiles of downwelling irradiance and upward radiance. First depth is 5 m, rather than 0 m. Error bars denote standard error. c) Predicted reflectance of the lateral surface of an organism viewed horizontally in the solar azimuth using modeled light field. d) Predicted reflectance of the lateral surface of an organism viewed horizontally opposite the solar azimuth using modeled light field. Solar elevation is 80°.

tive cases. When viewed in the solar azimuth, sighting distances were independent of solar elevation and weakly dependent on depth. When viewed opposite the solar azimuth, the sighting distances were higher, and these values were substantially higher at sunset. Organisms cryptic at 50-m depth had sighting distances that were strongly dependent on depth and longer at sunset. Specularly reflective organisms viewed in the solar azimuth were not cryptic, even at the 50-m depth for which they were optimized.

Discussion

General—The results of the current study support three major conclusions. First, both colored and mirrored organisms that are optimally cryptic under one set of viewing conditions (i.e., having zero contrast) become quite visible when viewed under different conditions. The sighting distances under different viewing conditions were on the order of 5–10 m for large organisms and 0.5–1.0 m for smaller organisms. This is in sharp contrast with benthic crypsis. A benthic organism that has a reflectance spectrum matching the substrate remains maximally cryptic under changes in water type, depth, solar elevation, and viewing angle and azimuth. Second, neither mirroring nor coloring was clearly a more robust cryptic strategy under varying viewing conditions. Mirrored organisms generally had shorter sighting distances when viewed under nonoptimal conditions but also could never be completely cryptic when viewed in the solar azimuth, because the predicted reflectance for zero inherent contrast was greater than one. Third, the depth-dependent variation in the optical properties of the water [$c(\lambda)$ and $K_L(\lambda)$] was important for large organisms but not for small organisms, where the $1/d^2$ term in Eq. 3 dominated the calculation of the sighting distance. For example, the sighting distances from the mismatch calculations were often proportional to depth for large organisms, because of the clearer water at depth, but generally inversely proportional to depth for small organisms as a result of the increasing minimum contrast threshold at lower levels of illumination.

It is important to note, however, that both strategies are highly successful when viewed under the conditions for which they have presumably been optimized. Either strategy can result in an organism that is indistinguishable from the background, even at very close range. The following dis-

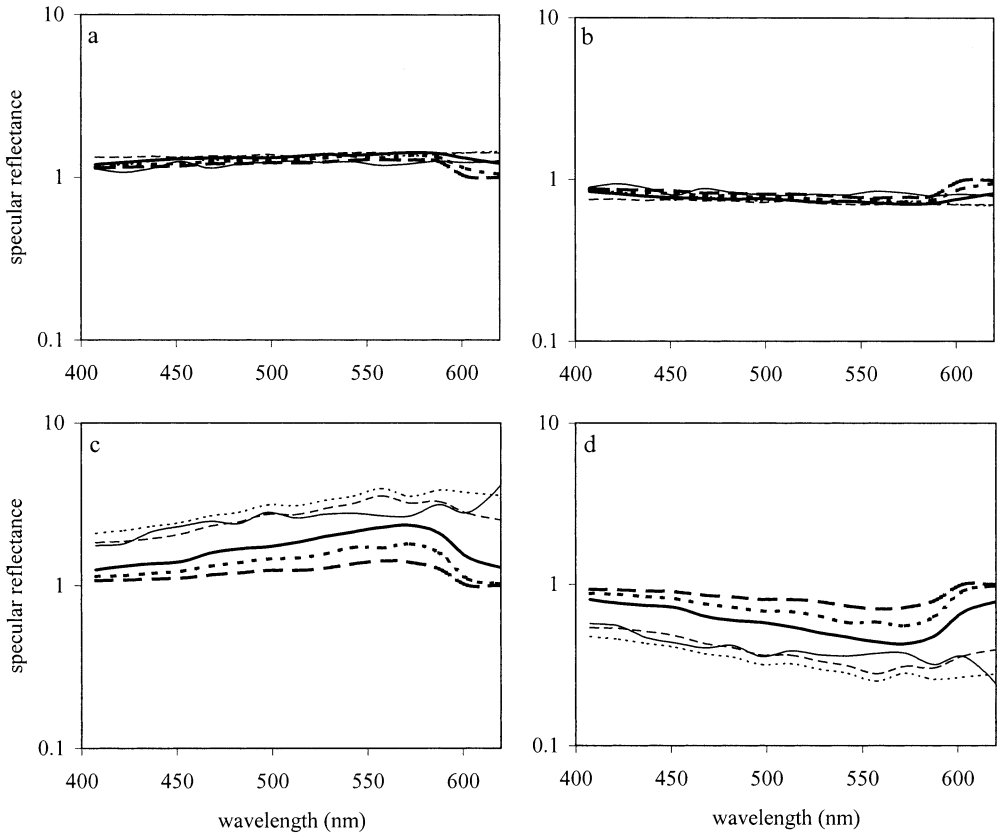

Fig. 4. Predicted specular reflectance spectra of a maximally cryptic organism using modeled light field. a) Predicted reflectance of the lateral surface of an organism viewed horizontally in the solar azimuth. b) Predicted reflectance of the lateral surface of an organism viewed horizontally opposite the solar azimuth. Solar elevation in a and b is 80°. c) Predicted reflectance of the lateral surface of an organism viewed horizontally in the solar azimuth. d) Predicted reflectance of the lateral surface of an organism viewed horizontally opposite the solar azimuth. Solar elevation in c and d is 10°.

cussion of the relative success of diffuse and specular reflection refers to their relative robustness under varying optical conditions. If organisms can slightly alter their coloration and reflective properties under changing optical conditions, as counterilluminating organisms can, both strategies can result in nearly perfect camouflage.

Effects of depth—The analysis predicted dark brown dorsal surfaces and either greenish-brown or highly reflective but colorless lateral surfaces. This generally matches what is observed in many coastal nekton (Cott 1940; Hardy 1959), suggesting that the assumptions underlying the calculations are reasonable. Unfortunately, aside from a few measurements of mirrored fish showing high specular reflectance (e.g., Rowe and Denton 1997), there appear to be no published measurements of the spectral reflectance of pelagic coastal organisms.

Both large and small organisms that were cryptic at 50-m depth had significant sighting distances at other depths, regardless of the viewing angle. As might be expected, the visibility generally increased in proportion to how much shallower the organism was compared to its optimal depth of 50 m. Normalizing for body length, the large organisms had roughly twice the sighting distances of the small organisms, implying that crypsis is more challenging for the former. Small mirrored organisms generally had slightly lower sighting distances than did colored organisms, because ideal reflectance was more or less independent of depth. However, mirrored organisms viewed in the solar azimuth could not be fully cryptic at any depth (because it required a reflectance higher than one). For large organisms, the visibilities of mirrored and colored organisms were roughly equally affected by being viewed at a different depth.

Dorsal surfaces—Viewing from above appears to be most constant of the three angles studied. The mismatch calculations showed that cryptic dorsal coloration was the least dependent on time of day and depth. This was not due to smaller contrast mismatches but rather to three other factors. First, the dorsal surface was viewed against the relatively dim upward radiance, so the minimum contrast threshold for the viewer was higher than it would be if it was viewing the lateral surface. More importantly, the attenuation of contrast in the downward viewing angle was higher than in the other viewing angles. The attenuation coefficient for contrast is $c(\lambda) - K_L(\lambda)$. Because the background radiance increases as

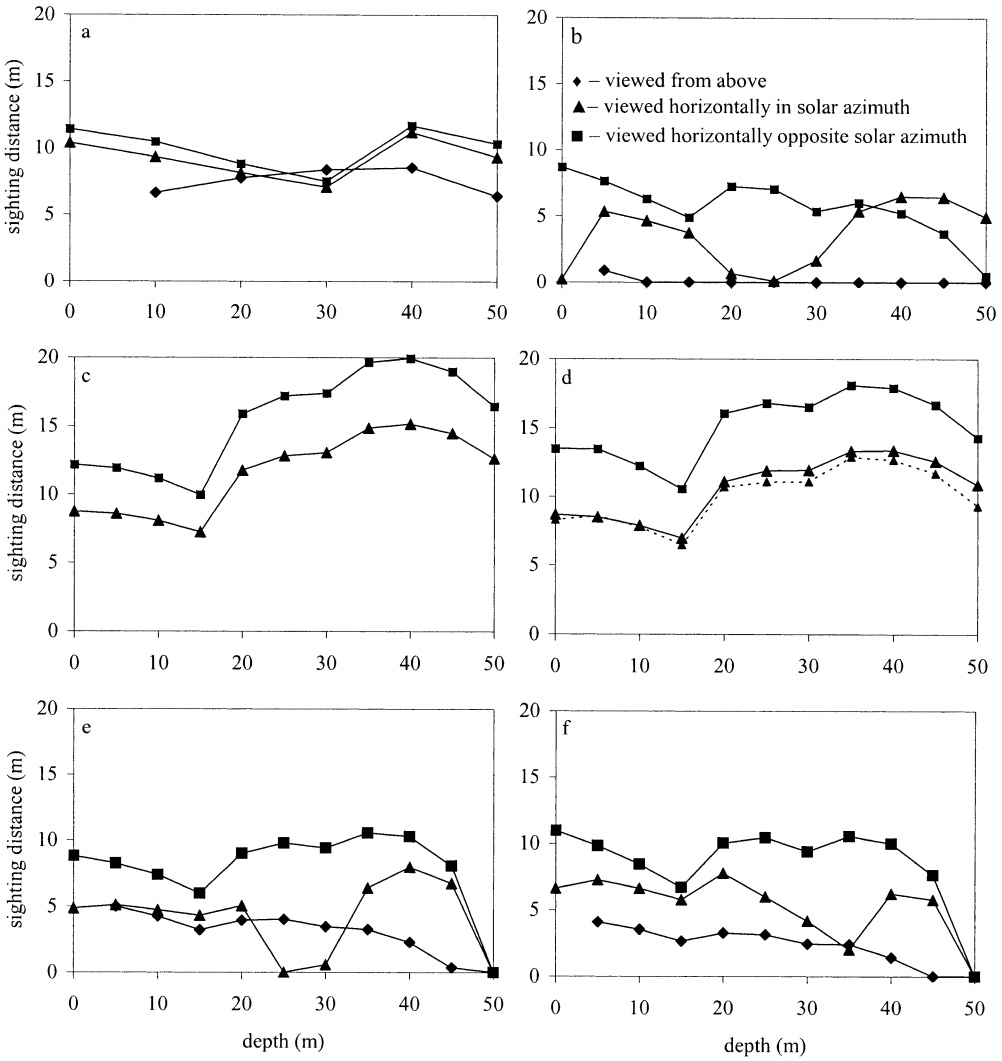

Fig. 5. Sighting distances of a 1-m–long, diffusely reflective organism cryptic in one situation viewed in a different situation. a) Organism cryptic in oceanic water viewed in coastal water (both near noon). b) Organism cryptic near noon viewed near sunset. c) Organism cryptic in one azimuth viewed horizontally in the opposite azimuth near noon. d) Organism cryptic in one azimuth viewed horizontally in the opposite azimuth near sunset. e) Organism cryptic at 50 m viewed at a shallower depth near noon. f) Organism cryptic at 50 m viewed at a shallower depth near sunset. Dotted line in d denotes the sighting distance determined using Eq. 9 rather than the simpler Eq. 1. No data are given at 0 m for the downward viewing angle, since this would place the viewer out of the water.

the viewer moves upward and away from the organism, $K_L(\lambda)$ is negative, and so the contrast attenuation coefficient is higher than it is at any other viewing angle (see Johnsen 2002). Finally, because the dorsal surface faces the entire hemisphere of the sky, it is less affected by changes in the position of the sun than are the lateral surfaces. The one situation in which the dorsal surface does not have an advantage over the lateral surfaces is in the case of changing water type. A dorsal surface that is cryptic in oceanic water is just as vulnerable to detection in coastal water as are lateral surfaces.

Lateral surfaces—As mentioned above, lateral surfaces are more vulnerable to detection under changing conditions, because the underwater light field at shallow depths is seldom symmetric. Even mirrored lateral surfaces, which are perfectly cryptic in a cylindrically symmetrical light field (Denton 1970), are visible in an asymmetric field when viewed at different azimuths. This is attributable to the fact that viewing in the solar azimuth increases the background radiance and decreases the organism's radiance, as a result of the lower irradiance or radiance at its surface. The reverse is true for viewing opposite the solar azimuth. Indeed, the mismatch calculations showed that organisms cryptic in one azimuth were quite visible when viewed in the opposite azimuth or at a different time of day.

Mirrored lateral surfaces were less vulnerable than colored surfaces to azimuthal changes, but they are slightly more

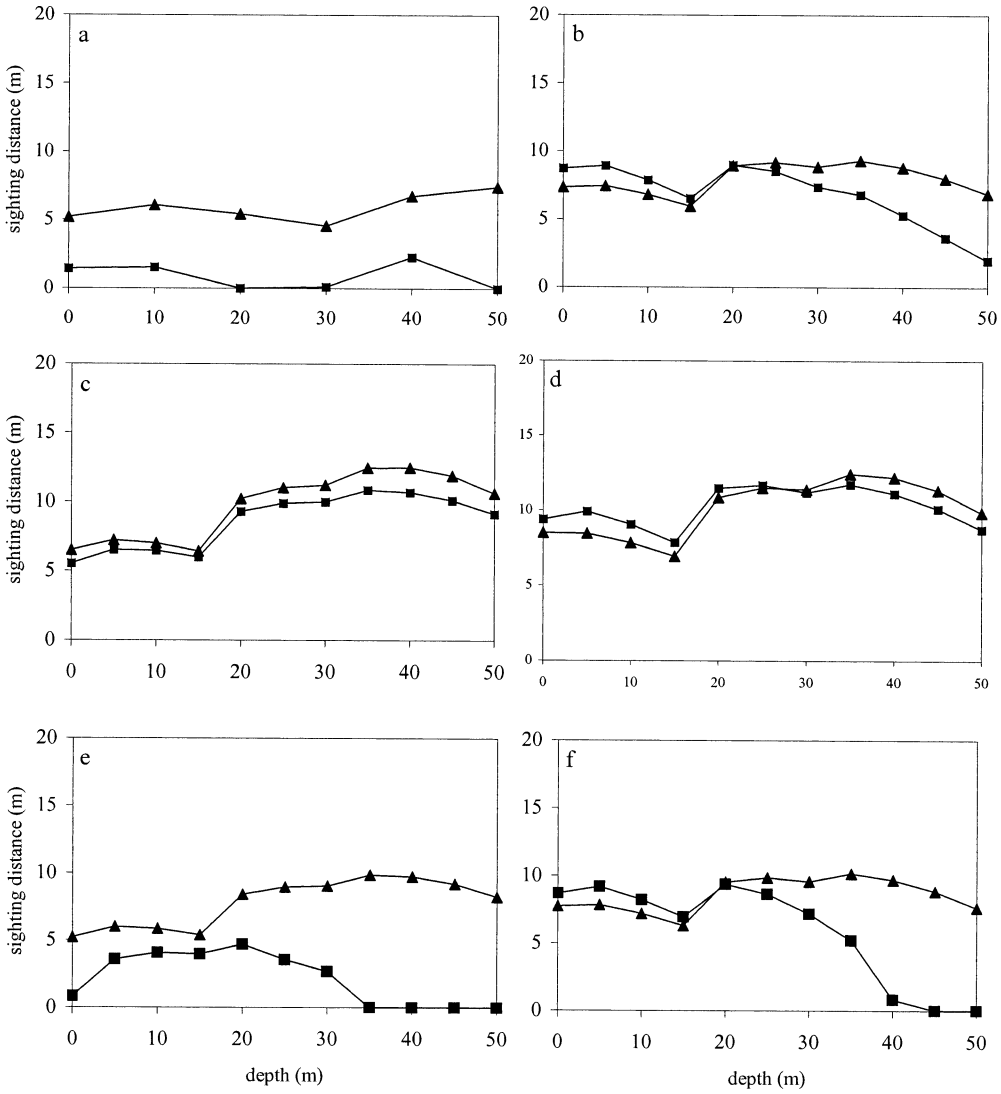

Fig. 6. Sighting distances of a 1-m–long, specularly reflective organism cryptic in one situation viewed in a different situation. See Fig. 5 for further details.

vulnerable to changes in solar elevation. However, because in actuality mirrored organisms will have curved surfaces, they have an additional issue to contend with. As a result of this curvature, there will be some position on the organism that will specularly reflect direct sunlight to the eye of the viewer, creating a bright flash. This is particularly important near the surface, where sunlight is still quite directional. Interestingly, certain species of mirrored pelagic fish appear to have compensated for this by organizing the reflective structures within the scales so that they are vertical regardless of the orientation of the scale (Denton 1970). Thus, a curved fish acts optically like a vertical mirror. It is unknown how common this strategy is among fish and other specularly reflective aquatic organisms.

Although upward viewing predominates at deeper depths (Muntz 1990), horizontal viewing is the most common at shallow depths. One reason for this may be the temporal and spatial complexity of the overhead light field near the surface. Wave-induced lensing of light results in rapid (1–100-Hz), large-scale fluctuations in light intensity and distribution. Internal reflection at the air–water interface and the possible presence of clouds also complicate the background for viewers attempting to detect predators or prey from below. A final reason may be the vulnerability of lateral surfaces to detection under changing viewing azimuths and solar elevations.

The azimuthal issue is particularly difficult to overcome. While organisms can control their depth, habitat, and the time of day at which they are active, they generally cannot control the azimuth from which they are viewed. As can be seen from the current study, the light field is still not symmetrical at a depth of 50 m. One possible compensation strategy is orientation parallel to the solar azimuth. In this orientation, the relatively large flanks of the organism receive equal illumination and can be simultaneously cryptic. This orientation also minimizes the effects of wave-induced lensing on the lateral surfaces. Certain fish species are known to orient and migrate using a solar compass (e.g.,

Table 1. Ranges of sighting distances of a 6-mm–long organism cryptic under one set of optical conditions but viewed under another set. Ranges in parentheses are for specularly reflective organisms. Ranges without parentheses are for diffusely reflective organisms. Ranges for one form of reflection that are significantly shorter than those for the other are in bold type.

Mismatch condition	Viewing angle	Sighting distance (cm)			
Cryptic in open ocean, viewed near coast	From above	83–37			
	In solar azimuth	90–35	**(38–27)**		
	Opposite solar azimuth	110–35	**(14–0)**		
Cryptic at noon, viewed at sunset	From above	15–0			
	In solar azimuth	**32–18**	(50–23)		
	Opposite solar azimuth	66–10	(67–13)		
		Noon		Sunset	
Cryptic in one azimuth, viewed in another	In solar azimuth	65–46	**(48–36)**	65–37	(62–33)
	Opposite solar azimuth	130–70	**(42–30)**	160–55	**(82–29)**
Cryptic at 50-m depth, viewed shallower	From above	52–0		65–0	
	In solar azimuth	**29–0**	(38–27)	**49–0**	(55–25)
	Opposite solar azimuth	67–0	**(27–0)**	100–0	**(71–0)**

Levin et al. 1992), but it is not known whether any species employ azimuthal orientation as a cryptic strategy.

Solar elevation—For colored organisms, the effect of solar elevation on crypsis was relatively small compared with other factors. Mirrored organisms were more affected, but not to a dramatic extent. This is due to the fact that, although the overall radiant intensity is strongly affected by solar elevation, the radiance distribution is affected less than might at first be suspected. This is primarily the result of three optical factors. First, refraction at the air–water interface decreases the range of solar elevations from 0–90° to 42.5–90°. Second, strong light absorption by the water implies that, as depth increases, the brightest point in the underwater light field migrates toward the zenith (which has the shortest optical path length). Third, light scattering by particles and the water itself results in a more diffuse light field. Because it is the radiance distribution and not the total light intensity that effects the predictions for crypsis, these three factors limit the effects of solar elevation on the predictions.

Although the results of the current study appear to be at odds with numerous studies describing the changing spectrum at twilight and its effects on visual predation (reviewed by McFarland et al. [1999]), this is because these studies involved light levels low enough to strongly affect contrast thresholds and spectral sensitivities (Douglas and Hawryshyn 1990). The light levels in this study were all above the photopic threshold of *G. morhua.* Below this threshold the contrast threshold and spectral sensitivity of *G. morhua* change dramatically (Anthony 1981; Anthony and Hawkins 1983).

Water type—The mismatch calculations showed that colored organisms that were cryptic in oceanic water became visible if they moved into coastal water. The effect was not as dramatic as that seen in the mismatch of azimuth, but it was more pronounced than the effect resulting from solar elevation. Whereas some species are confined to either coastal or oceanic waters, many are found in both types at various life stages, classic examples being salmonids and various species of eels. Countless studies have shown that many aquatic species change color to match various benthic backgrounds. In pelagic systems, other studies have shown that certain species change color depending on depth or time of day (e.g., Herring and Roe 1988). In addition, eel, sea lamprey, and certain salmon develop mirrored sides before venturing from freshwater into the ocean (reviewed by Herring [1994]). However, no study has examined color changes in pelagic organisms as a cryptic response to changes in water type.

Even organisms that never leave coastal water are subject to large variations in their optical environment because of changing phytoplankton levels, influxes of freshwater and sediment from rivers, eutrophication from agricultural runoff, and numerous other factors. These variations have significant effects on both visual predation and visual communication and, eventually, on the species composition of the ecosystem (e.g., Seehausen et al. 1997). These studies have generally focused on the viewer. None have examined whether the viewed species alter their coloration to compensate for these variations.

Mirrors versus colors and general implications for crypsis, foraging, and predator avoidance—Many pelagic organisms appear to be cryptically colored. Others, particularly teleost fish, have mirrored lateral surfaces. Most likely have reflectances intermediate between completely diffuse and specular. By examining the two extremes, this study attempted to determine the relative advantages and disadvantages of each strategic ideal. Mirrored surfaces appear to be cryptic over a wider range of optical environments than are diffusely reflective colored surfaces. Changes in viewing azimuth and water type had less effect on the crypsis of mirrored organisms. Changes in depth also had little effect, but this advantage was offset by the fact that mirrored surfaces could not be fully cryptic when viewed against the sun because of the high background radiance relative to the radiance incident on the surface. Mirrored organisms were also more affected by the time of day and are vulnerable to detection due to glinting reflections. Neither strategy clearly outperforms the

other. Perhaps the clearest result from the study is that both strategies have serious weaknesses in shallow water, particularly when the light field is asymmetric.

The most obvious implication for a cryptically colored or mirrored organism is that in order to remain cryptic, it must either have the capacity to change its color rapidly or it must limit the optical conditions under which it is viewed. As mentioned above, the latter is only possible at depths in which the light field is more symmetrical. Below this depth, the effects of depth, solar elevation, and viewing azimuth are negligible, and the organism can optimize its reflectance for different viewing angles, although the ventral surface is problematic (Johnsen 2002). Above this depth, crypsis either by colored or mirrored surfaces is limited, which may help explain both the predominance of transparent species in near-surface pelagic habitats (Johnsen 2001) and the vertical migration of many colored and mirrored species (Lampert 1993).

For an organism attempting to detect a cryptic predator or prey organism, several search strategies present themselves. First, the strong azimuthal effect indicates a circular search strategy, particularly near sunset. An organism circling a volume of water is far more likely to detect a cryptic organism within that volume, because at some angle the reflectance of the cryptic individual will be highly mismatched for the viewing conditions. In general, searching at low solar elevations is likely to be more successful than at high elevations, despite the lower overall light levels. Finally, once an organism is detected, it is likely to become more visible if it is driven toward the surface. All three of these tactics are commonly observed in pelagic predators (Gallo Reynoso 1991; Similae 1997; McFarland et al. 1999), but, of course, all have additional benefits besides optical detection (Ikehara et al. 1978; Gallo Reynoso 1991; McFarland et al. 1999).

Although mentioned above, it bears repeating that while predicted cryptic reflectances are independent of the visual system of the viewer, departures from these optima have varying effects on an organism's visibility, depending on the species viewing it. For example, whereas the increase in predicted long-wavelength reflectance with depth may be irrelevant to cod, it may be critically important for a different viewing species with excellent vision in the red. The predictions in this study form a physical background that must be combined with particular visual parameters to make conclusions about specific cases.

However, the general robustness of mirrored versus colored surfaces with respect to changing viewing conditions and the inability of mirrored surfaces to be cryptic when viewed against the sun are relatively independent of the viewer. The first is attributable to the higher variability in the predicted diffuse reflectance compared to the predicted specular reflectance (Figs. 3, 4). The second is attributable to the fact that the horizontal radiance in the solar azimuth is always greater than the radiance opposite the solar azimuth. Although the magnitude of these effects depends on the spectral and contrast sensitivity of the viewer, some effect will always be present.

References

AKSNES, D. L., AND A. C. W. UTNE. 1997. A revised model of visual range in fish. Sarsia **82:** 137–147.

ANTHONY, P. D. 1981. Visual contrast thresholds in the cod *Gadus morhua* L. J. Fish Biol. **19:** 87–103.

———, AND A. D. HAWKINS. 1983. Spectral sensitivity of the cod, *Gadus morhua* L. Mar. Behav. Physiol. **10:** 145–166.

BARRY, K. L., AND C. W. HAWRYSHYN. 1999. Effects of incident light and background conditions on potential conspicuousness of Hawaiian coral reef fish. J. Mar. Biol. Assoc. UK **79:** 495–508.

CHIAO, C. C., T. W. CRONIN, AND D. OSORIO. 2000. Color signals in natural scenes: Characteristics of reflectance spectra and effects of natural illuminants. J. Opt. Soc. Am. A **17:** 218–224.

COTT, H. B. 1940. Adaptive coloration in animals. Methuen.

DENTON, E. J. 1970. On the organization of reflecting structures in some marine animals. Phil. Trans. R. Soc. Lond. B **258:** 285–313.

———, J. B. GILPIN-BROWN, AND P. G. WRIGHT. 1972. The angular distribution of the light produced by some mesopelagic fish in relation to their camouflage. Proc. R. Soc. Lond. B **182:** 145–158.

DOUGLAS, R. H., AND C. W. HAWRYSHYN. 1990. Behavioral studies of fish vision: An analysis of visual capabilities, p. 373–418. *In* R. H. Douglas and M. B. A. Djamgoz [eds.], The visual system of fish. Chapman and Hall.

ENDLER, J. A. 1991. Variation in the appearance of guppy color patterns to guppies and their predators under different visual conditions. Vision Res. **31:** 587–608.

GALLO REYNOSO, J. P. 1991. Group behavior of common dolphins (*Delphinus delphis*) during prey capture. Ana. Inst. Biol. Univ. Nacion. Auto. Mexico **62:** 253–262.

GREGG, W. W., AND K. L. CARDER. 1990. A simple spectral solar irradiance model for cloudless maritime atmospheres. Limnol. Oceanogr. **35:** 1657–1675.

HARDY, A. C. 1959. The open sea, its natural history: Fish and fisheries. Houghton Mifflin.

HARRISON, A. W., AND C. A. COOMBES. 1988. An opaque cloud cover model of sky short wavelength radiance. Sol. Energ. **41:** 387–392.

HERRING, P. J. 1994. Reflective systems in aquatic animals. Comp. Biochem. Physiol. **109A:** 513–546.

———, AND H. S. J. ROE. 1988. The photoecology of pelagic oceanic decapods. Symp. Zool. Soc. Lond. **59:** 263–290.

IKEHARA, W., J. ATEMA, A. BRITTAIN, J. BARDACH, A. DIZON, AND K. HOLLAND. 1978. Reactions of yellowfin tuna to prey scents. Pac. Sci. **32:** 97.

JOHNSEN, S. 2001. Hidden in plain sight: The ecology and physiology of organismal transparency. Biol. Bull. **201:** 301–318.

———. 2002. Cryptic and conspicuous coloration in the pelagic environment. Proc. R. Soc. Lond. B **269:** 243–256.

LAMPERT, W. 1993. Ultimate causes of diel vertical migration of zooplankton: New evidence for the predator-avoidance hypothesis. Arch. Hydrobiol. **39:** 79–88.

LEVIN, L. E., P. BELMONTE, AND O. GONZALEZ. 1992. Sun-compass orientation in the characid *Cheirodon pulcher*. Environ. Biol. Fish **35:** 321–325.

LINK, J. S., AND L. P. GARRISON. 2002. Trophic ecology of Atlantic cod *Gadus morhua* on the northeast US continental shelf. Mar. Ecol. Prog. Ser. **227:** 109–123.

MARSHALL, N. J. 2000. Communication and camouflage with the same ''bright'' colours in reef fish. Phil. Trans. R. Soc. Lond. B **355:** 1243–1248.

MCFARLAND, W. N., C. WAHL, T. SUCHANEK, AND F. MCALARY. 1999. The behavior of animals around twilight with emphasis on coral reef communities, p. 583–628. *In* S. N. Archer, M. B. A. Djamgoz, E. R. Loew, J. C. Partridge, and S. Vallerga [eds.], Adaptive mechanisms in the ecology of vision. Kluwer.

MERTENS, L. E. 1970. In-water photography: Theory and practice. Wiley.

MOBLEY, C. D., AND OTHERS. 1993. Comparison of numerical models for computing underwater light fields. Appl. Opt. **32:** 7484–7504.

———, L. K. SUNDMAN, AND E. BOSS. 2002. Phase function effects on oceanic light fields. Appl. Opt. **41:** 1035–1050.

MUNTZ, W. R. A. 1990. Stimulus, environment and vision in fishes, p. 491–511. *In* R. H. Douglas and M. B. A. Djamgoz [eds.], The visual system of fish. Chapman and Hall.

PALMER, J. M. 1995. The measurement of transmission, absorption, emission, and reflection, p. 25.1–25.5. *In* M. Bass, E. W. Van Strylan, D. R. Williams, and W. L. Wolfe [eds.], Handbook of optics II. McGraw-Hill.

PEGAU, W. S., D. GRAY, AND J. R. V. ZANEVELD. 1997. Absorption and attenuation of visible and near-infrared light in water: Dependence on temperature and salinity. Appl. Opt. **36:** 6035–6046.

POPE, R. M., AND E. S. FRY. 1997. Absorption spectrum 380–700 nm. of pure water. II Integrating cavity measurements. Appl. Opt. **36:** 8710–8723.

PRIEUR, L., AND S. SATHYENDRANATH. 1981. An optical classification of coastal and oceanic waters based on the specific spectral absorption curves of phytoplankton pigments, dissolved organic matter, and other particulate materials. Limnol. Oceanogr. **26:** 671–689.

ROWE, D. M., AND E. J. DENTON. 1997. The physical basis for reflective communication between fish, with special reference to the horse mackerel, *Trachurus trachurus.* Phil. Trans. R. Soc. Lond. B **352:** 531–549.

SEEHAUSEN, O., J. J. M. ALPHEN, AND F. WITTE. 1997. Cichlid fish diversity threatened by eutrophication that curbs sexual selection. Science **277:** 1808–1811.

SIMILAE, T. 1997. Sonar observations of killer whales (*Orcinus orca*) feeding on herring schools. Aquat. Mammals **23:** 119–126.

ZANEVELD, J. R. V., J. C. KITCHEN, AND C. C. MOORE. 1994. The scattering error correction of reflecting tube absorption meters. Proc. Soc. Opt. Eng. **2258:** 44–55.

Received: 20 May 2002
Accepted: 6 December 2002
Amended: 20 January 2003